Biochemical and Biophysical Research Communications 425 (2012) 886–891

Contents lists available at SciVerse ScienceDirect

Biochemical and Biophysical Research Communications

journal homepage: www.elsevier.com/locate/ybbrc

Synergistic enhancement of iron oxide nanoparticle and gadolinium for dual-contrast MRI

Fan Zhang [a,c], Xinglu Huang [a], Chunqi Qian [b,c], Lei Zhu [a,c], Naoki Hida [a], Gang Niu [a,*], Xiaoyuan Chen [a,*]

[a] Laboratory of Molecular Imaging and Nanomedicine (LOMIN), National Institute of Biomedical Imaging and Bioengineering (NIBIB), National Institutes of Health (NIH), Bethesda, MD 20892, USA
[b] Laboratory of Functional and Molecular Imaging, National Institute of Neurological Disorders and Stroke (NINDS), National Institutes of Health (NIH), Bethesda, MD 20892, USA
[c] Center for Molecular Imaging and Translational Medicine, School of Public Health, Xiamen University, Xiamen 361005, China

ARTICLE INFO

Article history:
Received 30 July 2012
Available online 7 August 2012

Keywords:
MRI
Gd-DTPA
Iron oxide
RGD
Dual contrast

ABSTRACT

Purpose: The use of MR contrast agents allows accurate diagnosis by exerting an influence on the longitudinal (T_1) or transverse (T_2) relaxation time of the surrounding tissue. In this study, we combined the use of iron oxide (IO) particles and nonspecific extracellular gadolinium chelate (Gd) in order to further improve the sensitivity and specificity of lesion detection.
Procedures: With a 7-Tesla scanner, pre-contrasted, IO-enhanced and dual contrast agent enhanced MRIs were performed in phantom, normal animals, and animal models of lymph node tumor metastases and orthotopic brain tumor. For the dual-contrast (DC) MRI, we focused on the evaluation of T_2 weighted DC MRI with IO administered first, then followed by the injection of a bolus of gadolinium diethylenetriamine pentaacetic acid (Gd-DTPA).
Results: Based on the C/N ratios and MRI relaxometry, the synergistic effect of coordinated administration of Gd-DTPA and IO was observed and confirmed in phantom, normal liver and tumor models. At 30 min after administration of Feridex, Gd-DTPA further decreased T_2 relaxation in liver immediately after the injection. Additional administration of Gd-DTPA also immediately increased the signal contrast between tumor and brain parenchyma and maximized the C/N ratio to -4.12 ± 0.71. Dual contrast MRI also enhanced the delineation of tumor borders and small lesions.
Conclusions: DC-MRI will be helpful to improve diagnostic accuracy and decrease the threshold size for lesion detection.

1. Introduction

Based on the interaction of protons with the surrounding molecules of tissues, magnetic resonance imaging (MRI) has been recognized as a powerful noninvasive diagnostic technique to visualize the fine structure of a human body in high spatial resolution [1]. The use of MR contrast agents enables achievement of clear images for accurate diagnosis, by exerting an influence on the longitudinal (T_1) or transverse (T_2) relaxation time of the surrounding tissue. Thermodynamically stable, water-soluble, and highly paramagnetic Gd(III) complexes have demonstrated high relaxivity and have therefore served as versatile T_1 positive contrast agents [2]. On the other hand, superparamagnetic iron oxide (SPIO) NPs with superior magnetic properties have emerged as a prevailing agent due to their strong T_2 shortening effect [3,4]. Dextran coated iron oxide NPs (such as Ferridex) have been approved by the Food and Drug Administration (FDA) for clinical use, particularly for detecting focal liver lesions [5–7].

Since the magnetite nanoparticles represent dark areas in MR images, their negative contrast is often confused with a low-level MR signal arising from adjacent tissues such as bone or vasculature [8]. Furthermore, susceptibility artifacts can occur as a result of the steep change of local magnetic field around iron oxide nanoparticles, leading to the locally distorted anatomy of surrounding tissue in MR image [9]. In order to improve the sensitivity and specificity of lesion detection, several studies have described the combined use of iron oxide particles and nonspecific extracellular gadolinium chelate (Gd) [10–12]. Dual-contrast (DC) MR imaging involves the administration of SPIO and gadopentetate dimeglumine contrast agents in the same imaging session. By combining the enhancement pattern of the nodules after gadolinium administration on one hand and the tissue-specific information obtained after SPIO administration on the other, this technique has been demonstrated to improve the detection of hepatocellular carcinoma (HCC) nodules [13,14].

* Corresponding authors. Addresses: 31 Center Drive, Suite 1C14, Bethesda, MD 20892-2281, USA (X. Chen), 10 Center Drive, B3B25, Bethesda, MD 20892-2281, USA (G. Niu).
E-mail addresses: niug@mail.nih.gov (G. Niu), shawn.chen@nih.gov (X. Chen).

0006-291X/$ - see front matter © 2012 Elsevier Inc. All rights reserved.
http://dx.doi.org/10.1016/j.bbrc.2012.07.168

It has been found that when both Gd-DTPA and ferrite particles were administered together, the tumor-liver contrast-to-noise (C/N) ratio magnitude reached a maximum at 12 min after drug infusion [12]. DC-MRI with combined use of chondroitin sulfate iron colloid (CSIC) and Gd-DTPA in patients with HCC also demonstrated that DC-MRI was significantly better than Gd-DTPA enhanced T_1WI and CSIC enhanced T_2WI in tumor detectability and depicting tumor spread [15]. Sequential use of ferumoxide particles and nonspecific extracellular gadolinium chelate (Gd) for evaluation of focal liver lesions on MRI revealed that Gd and ferumoxide can be administered sequentially within one study session without substantial loss of diagnostic information obtained on sequences performed after administration of the second contrast agent [11].

So far, most of DC-MRI studies were applied for lesion detection within the liver. In order to elaborate the synergistic effect of SPIO and gadolinium, in this study, we expanded the dual contrast enhanced MRI to lymph node metastasis and orthotopic brain tumor models after a phantom study.

2. Materials and methods

2.1. Contrast agents and phantom preparation

RGD conjugated IONPs were prepared according to the same procedure reported previously [16]. For phantom preparation, different amount of free Ferumoxides suspension (Feridex I.V., Bayer HealthCare Pharmaceuticals Inc., Wayne, NJ) was mixed with gadopentetate dimeglumine (Gd-DTPA Magnevist, Bayer Schering Pharma AG, Berlin, Germany) in 200 μl 0.8% agarose. The concentration gradient of Feridex ranges from 0 to 23.45 mg/ml and that of Gd-DTPA ranges from 0 to 1.5625 μg/ml. In a container with a diameter of 5 cm, six eppendorf tubes (0.8 cm in diameter) were embedded in 0.8% agarose. For in vivo imaging, Gd-DTPA is diluted in 0.9% NaCl to a concentration of 20 mM and injected in mice at a dose of 0.02 mmol/kg. Feridex is also diluted in 0.9% NaCl and injected in mice at a dose of 0.05 mmol Fe/kg.

2.2. Cell culture and animal model

Luciferase-expressing 4T1 murine breast cancer cells were maintained at 37 °C in a humidified atmosphere containing 5% CO_2 in Dulbecco's Modification of Eagles Medium (DMEM) with 10% fetal bovine serum (FBS) [17]. The human glioblastoma cell line U87MG was grown in DMEM medium supplemented with 10% FBS, 100 IU/ml penicillin, and 100 μg/ml streptomycin (Invitrogen), and in a humidified atmosphere containing 5% CO_2 at 37 °C.

All animal procedures were performed according to a protocol approved by the National Institutes of Health Clinical Center Animal Care and Use Committee (NIH CC/ACUC). The lymph node metastasis model was established in 4–6 week-old female BALB/c mice by subcutaneous injection of 0.5×10^6 of 4T1-Luc cells to the hock of the right leg of mice [17]. At day 14 to day 28 after cell inoculation, tumor bearing mice ($n = 5$ each group) underwent bioluminescent imaging every three days to monitor tumor metastasis to lymph nodes.

Orthotopic brain tumor model was established by stereotaxic injection of 1×10^5 U87MG cells suspended in 5 μl phosphate-buffered saline (PBS). The female athymic nude mouse (nu/nu) at four to six weeks of age is placed in a stereotaxic jig made by Stoelting (Wood Dale, IL). After the surgical area was cleaned and prepared, an incision was made. The bregma was located to determine the location of the craniotomy. The location of the injection was 2 mm to the right and 0.5 mm rostral to the bregma. The depth was 3 mm from the surface of the skull. Tumor cells were allowed to engraft for 10 days, then MRI were performed weekly to assess tumor growth.

2.3. MRI

All experiments were performed on a 7 T MRI scanner (Bruker, Germany) equipped with a single channel head coil for signal reception.

For phantom acquisition, images were acquired with the phantom parallel to the B_0 direction using the following parame-

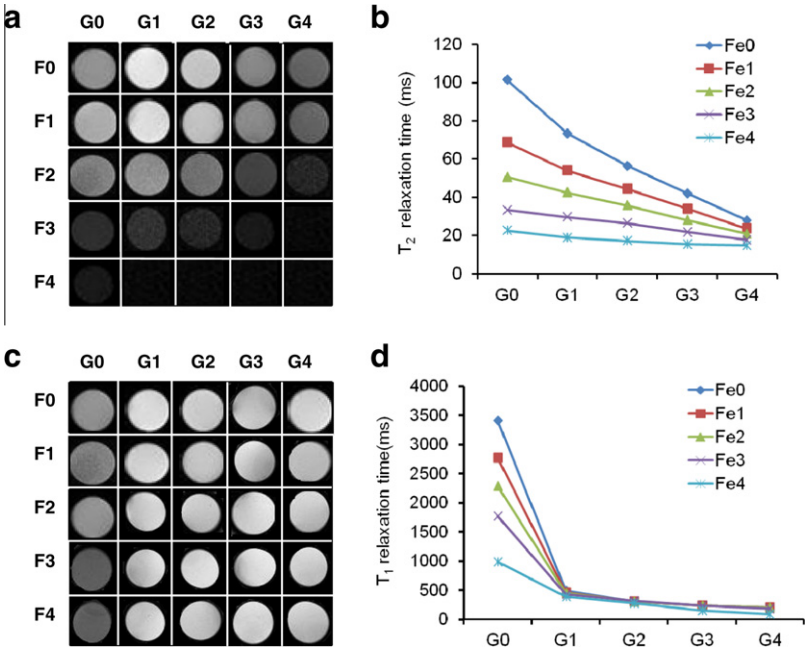

Fig. 1. MRI imaging of the phantoms. For phantom preparation, different amount of free Ferumoxides suspension was mixed with Gd-DTPA in 200 μl 0.8% agarose. G0 to G4 stand for the concentration gradient of Gd-DTPA ranging from 0 to 1.56 μg/ml (2-fold serial dilution) while F0 to F4 stand for the concentration gradient of Feridex ranging from 0 to 23.45 mg/ml (2-fold serial dilution). (A and B) T_2-weighted MRI; (C and D) T_1-weighted MRI.

ters: T_1-weighted multislice gradient-echo images: TR/TE = 250/4.5 ms, matrix = 256 × 256, FA = 30, 9 contiguous slices; T_2-weighted multislice spin-echo images: TR/TE = 2000/48 ms, matrix = 256 × 256, 9 contiguous slices; T_2-map: TR = 2000/48 ms, matrix = 256 × 256, 1 slices, T_2 relaxation measurements with TE from 10 to 160 ms; T_1 relaxation measurements were acquired with TR of 120, 273, 454, 674, 957, 1354, 2021 and 5000 ms with a TE of 56 ms. All images had a 35 mm × 35 mm field of view. The T_2 and T_1 values of each phantom were calculated using the fitting function provided by the manufacture software.

Different mouse data sets were acquired using a 4 cm receive-only RF coil. Mice were anesthetized via inhalation of isoflurane (1.5–2%) in O_2. During the experiment, the temperature of the animal was maintained at 37.0 ± 0.5 °C with the use of a circulating warm water (37 °C) blanket. The respiration rate was monitored with an optical sensor of motion. All scan parameters were similar to those of the phantom scan. All animals were imaged with T_1- and T_2-weighted pulse sequences before administration of contrast agents. Sequential administration of Feridex and Gd-DTPA was performed for dual-contrast MRI. For lymph node imaging, a catheter was inserted in a foot pad to allow administration of the contrast agents. In one group of mice, Feridex was injected at 15 min after administration of Gd-DTPA. In another group, Gd-DTPA was injected into the animals 30 min after administration of iron oxide. Gd-DTPA and iron oxide contrast agents were administered at a dose of 0.2 mmol/kg and 0.05 mmol Fe/kg, respectively, in a volume of 20 μl PBS through the foot pad.

For liver imaging, a catheter was inserted into a lateral tail vein of mice. After catheter insertion, the animal was placed on a custom-made plastic cradle. Gd-DTPA was injected into the same animals 30 min after administration of iron oxide. Gd-DTPA and iron oxide contrast agent is administered at a dose of 0.2 mmol/kg and 0.05 mmol Fe/kg in a volume of 200 μl PBS respectively via injection into the tail vein.

For brain tumor imaging, 0.2 mmol/kg of Gd-DTPA was injected intravenously into the same animals 2 h after administration of IO-RGD at a dose of 0.05 mmol Fe/kg. The images were acquired immediately before, immediately after and 1 h after GD-DTPA administration. The transverse relaxation rates and contrast-to-noise (C/N) ratios were then measured.

2.4. Image analysis

For phantom and animal liver study, MRI T_2 relaxometry was calculated. For lymph node tumor metastasis and brain tumor models, quantitative analysis of the reference lesions was performed by operator-defined regions of interest (ROIs). Signal intensities of the normal lymph node, the reference lymph node lesion, brain parenchyma, the reference brain tumor and the background were measured in each animal for all sequences before and after contrast administration. Then the C/N ratio was calculated with following formula:

$$C/N_{\text{lymph node}} = (SI_{\text{nomal lymph node}} - SI_{\text{tumor metastasis}})/\text{background noise}$$

$$C/N_{\text{brain tumor}} = (SI_{\text{tumor}} - SI_{\text{brain parenchyma}})/\text{background noise}$$

The C/N ratio is an effective parameter for quantitating MR pulse sequence performance, as the absolute magnitude of C/N, designated as [±C/N ratio], correlates with lesion detectability. It follows from equation that negative C/N values indicate relatively hypointense (dark) pathology. Values near zero denote iso-intensity and poor lesion conspicuity [12,18].

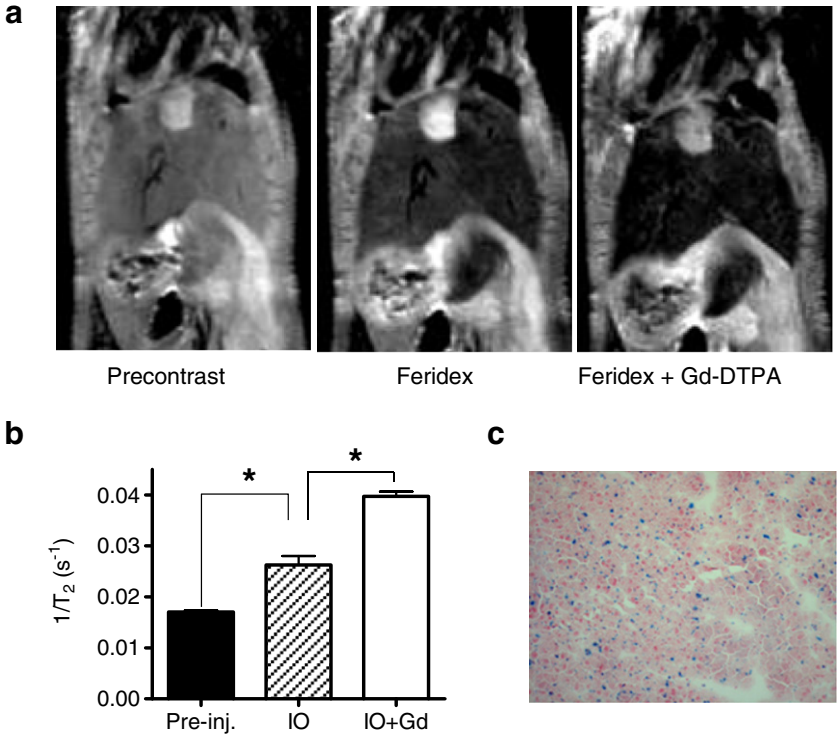

Fig. 2. Dual-contrast T_2-weighted MRI of normal livers. (A) T_2-weighted MRI of a mouse before contrast agent administration (left), 30 min after iron oxide nanoparticles administration (middle) and after administration of Gd-DTPA at 30 min after administration of IO nanoparticles (right). (B) Transverse relaxation rates of live after administration of IO and Gd-DTPA. (C) Prussian blue staining of liver tissue.

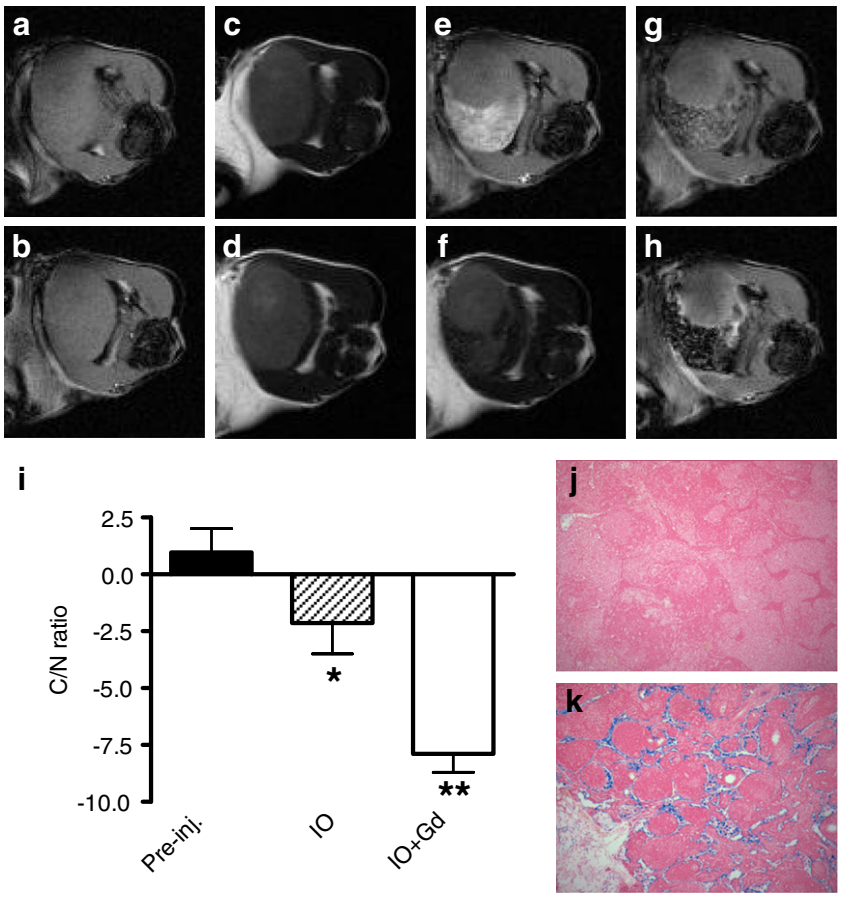

Fig. 3. Dual-contrast MRI of lymph node metastases. (A and B) Unenhanced T_1-weighted MRI with fast low-angle shot (FLASH) sequence. (C and D) Unenhanced T_2-weighted MRI with tuber fast spin echo sequence. (E) T_1-weighted MRI immediately after administration of Gd-DTPA. (F) T_2-weighted MRI at 30 min after iron oxide nanoparticles administration. (G) T_2-weighted dual contrast MRI with Gd-DTPA first then IO. (H) T_2-weighted dual contrast MRI with IO first then Gd-DTPA. (I) Contrast-to-noise (C/N) ratios calculated based on the signal intensity over the lymphatic tissue and metastatic tumor tissue. (J and K) Prussian blue staining of lymphatic tissue (J) and metastatic tumor tissue (K) within the lymph node.

2.5. Statistical analysis

A Student's *t*-test was performed to determine if there was a significant difference in C/N ratio. *P*-values of less than 0.05 were considered statistically significant.

3. Results

3.1. Phantom study

To validate the changes of relaxation rate of the mixed contrast agent, we prepared phantom by mixing different concentrations of Gd-DTPA and Feridex in 200 μl 0.8% agarose. Then T_1- and T_2-weighted MR images were acquired and relaxation rates were measured. As shown in Fig. 1, increased Gd-DTPA concentrations without changing the iron oxide concentration can induce a negative signal enhancement on the T_2-weighted images. This phenomenon is more prominent with low concentrations of iron oxide. At the same time, iron oxide barely enhances the signal intensity even at relatively high concentration range.

3.2. Liver imaging

Feridex is a reticuloendothelial system (RES) specific intracellular superparamagnetic contrast agent and the particles are selectively phagocytosed by hepatic Kupifer cells, decreasing signal intensity of normal liver but not the tumor. Consequently, most of DC-MRI studies focused on lesion detection in the liver. As shown in Fig. 2, Feridex enhanced the conspicuity of the whole liver. At 30 min after administration of Feridex, Gd-DTPA further decreased T_2 relaxation in the liver immediately after the injection. T_2 relaxivity of DC-MRI is significantly higher than that of Feridex enhanced MRI ($P < 0.05$) (Fig. 2B). The iron oxide particle accumulation inside the liver was confirmed by positive Prussian blue staining (Fig. 2C).

3.3. Lymph node imaging

Local injection of contrast agent is the most common route for lymph node imaging. Enlarged tumor draining lymph nodes are detectable on both precontrast T_1- and T_2 weighted MRI. However, virtually no contrast between tumor and healthy lymph node tissue was identified. Gd-DTPA injection resulted in a profound signal increase of surrounding lymph node tissue in contrast to the metastatic tumor. Administration of Feridex decreased signal intensity in healthy lymph node tissue while tumor signal intensity did not change. At 30 min after Feridex injection, administration of Gd-DTPA increased tumor signal intensity while did not affect the signal loss in lymphatic tissue (Fig. 3). Consequently, the dual contrast MRI further increased the C/N ratio to -7.89 ± 0.82, which is significantly higher than that of Feridex only (-2.14 ± 1.36, $P < 0.05$).

Prussian blue staining revealed that iron oxide was mainly distributed in medullary sinuses in lymphatic tissue, which contrib-

uted to the locally reduced signal intensity. Metastatic tumor cells showed minimal iron oxide uptake, which corresponds to the region without signal reduction.

3.4. Brain tumor imaging

On precontrast T_2 weighted MRI, orthotopic U87MG tumor presented higher signal intensity than peripheral brain parenchyma, as shown in Fig. 4A. At 2 h after intravenous injection of RGD peptide conjugated IO decreased tumor signal intensity in contrast to brain parenchyma, indicating distribution of RGD-IO in the tumor region. However, there is not significant decrease of the C/N ratio compared with the precontrast MRI ($P > 0.05$). Additional administration of Gd-DTPA immediately increased the signal contrast between tumor and brain parenchyma and maximized the C/N ratio to -4.12 ± 0.71. At 1 h after Gd-DTPA injection, the signal contrast was lost and the C/N ratio was restored.

More importantly, dual contrast MRI further enhanced the delineation of tumor borders and small lesions. As is shown in Fig. 4J, two satellite lesions were visualized clearly with dual contrast MRI, which were ambiguous on both precontrast MRI and IO-RGD enhanced MRI (data no shown). HE staining confirmed the existence of malignant lesions.

4. Discussion

Superparamagnetic iron oxide (SPIO) contrast agents have been intensively applied in the identification and characterization of focal hepatic lesions [19,20]. Dynamic MRI following a bolus injection of paramagnetic Gd-DTPA is another widely used technique to study liver cirrhosis and characterize HCC [21]. Dual contrast MRI which combines both SPIO and Gd-DTPA has been reported to improve the diagnostic accuracy of MRI in the study of focal hepatic lesions [10,22]. They found that the small areas of arterial-phase enhancement with Gd-DTPA that fail to take up SPIO are always HCC. Consequently, the main advantage of DC-MRI for HCC detection lies in that decreased contrast between tumor and the liver parenchyma caused by Gd-DTPA administration is increased by simultaneous use of iron oxide which reduces signal intensity of the liver tissue surrounding the tumor.

As to the sequential use of ferumoxide particles and Gd-DTPA for the evaluation of focal liver lesions on MRI, Semelka et al. [11] studied the order of contrast administration and imaging effect of the first contrast agent on sequences acquired after the second contrast agent. With ferumoxide first, a synergistic effect of decreased signal intensity of normal liver background with ferumoxide particles and increased signal intensity of liver lesions with Gd was identified on Gd-enhanced SGE images. This phenomenon also has been identified with T_1-weighted spin-echo images in rats [12].

With phantom, we observed that increased Gd-DTPA concentrations without changing the iron oxide concentration can induce a negative signal enhancement on the T_2-weighted images, especially with low concentration of iron oxide (Fig. 1). The possible explanation lies in that Gd^{3+} has seven unpaired electrons with high paramagnetic susceptibility, and it can enhance the local field gradient that was originally introduced by the superparamagnetic nanoparticles. Thus, in this study, we focused on the evaluation of T_2 weighted dual contrast MRI with SPIO, expanding from normal liver to tumor metastatic lymph nodes and brain tumor models. There is no surprise to observe decreased signal intensity on T_2-weighted MRI after *i.v.* injection of SPIO (Fig. 2), due to the fact that the heterogeneous distribution of superparamagnetic nanoparticles introduces a big local field gradient that can be sensed by Gd^{3+}.

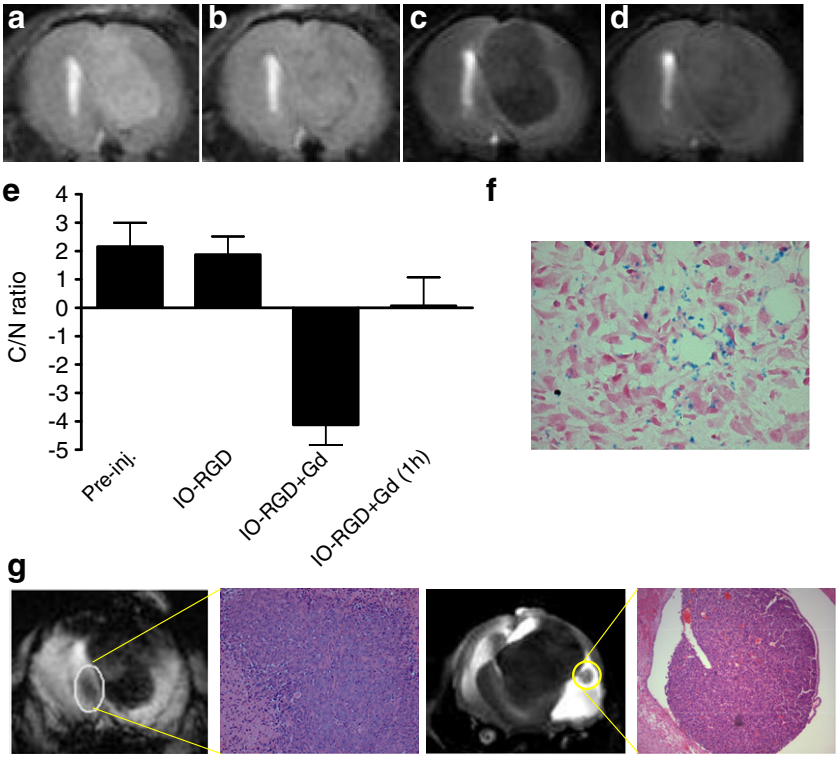

Fig. 4. Dual contrast MRI of othortopic brain tumors. (A) T_2-weighted precontrast MRI. (B) T_2-weighted MRI at 2 h after IO-RGD administration. (C) Dual contrast T_2-weighted MRI immediately after Gd-DTPA administration. (D) Dual contrast T_2-weighted MRI immediately at 1 h after Gd-DTPA administration. (E) Contrast-to-noise (C/N) ratios calculated based on the signal intensity over the normal brain tissue and tumor tissue. (F) Prussian blue staining of brain tumor tissue. (G) Representative dual contrast T_2-weighted MRI for delineation and detection of small lesions.

Contrast enhanced MR lymphography (CE-MRL) is a noninvasive method that offers a high contrast and spatial resolution [23]. Interstitial administration of lymphographic contrast media such as SPIO [24,25] allows high accumulation in regional lymph nodes. Consistent with previous studies [25], we also observed that administration of Feridex decreased signal intensity in healthy lymph node tissue while tumor signal intensity did not change. Dual contrast MRI with Feridex injection first followed by administration of Gd-DTPA further increased tumor signal intensity without affecting the signal intensity in the lymphatic tissue (Fig. 3). The synergistic effect may be beneficial to increase conspicuity of tumor metastases in lymph nodes. After interstitial injection, SPIO particles are taken up into highly permeable, thin walled and fenestrated lymphatic capillaries, and transported with the lymph fluid to the lymph nodes and taken up by macrophages in the nodes [26]. Metastatic tumors inside the lymph node showed minimal uptake of SPIO as confirmed by Prussian blue staining. In contrast, Gd-DTPA is more diffusible to the whole region of lymph nodes, which may include the metastatic lesions [27]. By administering Gd-DTPA first, no appreciable effect on the iron oxide-enhanced T_2-weighted images was observed (data not shown). We speculated that it may be due to the much faster clearance rate of Gd-DTPA than SPIO.

The integrin $\alpha_v\beta_3$ receptor is upregulated on both tumor cells and the endothelium, and it plays important roles in metastasis and angiogenesis [28]. Various imaging methods have been tried to visualize and quantify integrin expression in both preclinical animal models and clinical settings [29,30]. We have visualized tumor targeting of the integrin $\alpha_v\beta_3$ specific contrast agent, IONP-RGD via MRI. With lower dose of IONP-RGD, we observed dropped signal intensity in tumor region compared with brain parenchyma. However, the signal contrast is not ideal (Fig. 4). A bolus injection of Gd-DTPA significantly increased the lesion conspicuity and C/N ratio. In particular, this method further delineated the border of the malignant tumors, which is helpful in identifying small lesions. At 1 h after Gd-DTPA injection, the signal enhancement and tumor contrast was ambiguous due to the fast clearance of Gd-DTPA.

Besides the signal enhancement of Gd^{3+} to SPIO, the distinct pharmacokinetic distribution of SPIO and Gd-DTPA further increased C/N ratios with different administration routes in different models. For example, in the case of tumor metastasis in lymph nodes, interstitial injection of the contrast agents facilitated accumulation of SPIO by macrophages in normal lymphatic tissues. On the other hand, Gd-DTPA is more diffusive to tumor tissue and enhanced the signal intensity in metastatic tumors. In the case of orthotopic brain tumor, normal brain parenchyma showed almost no SPIO uptake comparing with tumor tissues. Administration of Gd-DTPA further decreased signal intensity in tumors while increased signal intensity of normal brain in T_2 weighted images.

To conclude, the synergistic effect of dual contrast MRI is a result of two contributions. One is from the high paramagnetic susceptibility of Gd^{3+}-enhanced local field gradient and the other is due to the distinct pharmacokinetic distribution of SPIO and Gd-DTPA. This synergistic effect of coordinated administration of Gd-DTPA and IO was observed and confirmed in phantom, normal liver and tumor models. This strategy will be helpful to improve diagnostic accuracy and decrease the threshold size for lesion detection.

Acknowledgments

This work was supported by the Intramural Research Program of the National Institute of Biomedical Imaging and Bioengineering (NIBIB), National Institutes of Health (NIH). F. Zhang is partly supported by the National Science Foundation of China (NSFC) (81201086).

References

[1] M. Rudin, R. Weissleder, Molecular imaging in drug discovery and development, Nat. Rev. Drug Discov. 2 (2003) 123–131.
[2] T.J. Meade, A.K. Taylor, S.R. Bull, New magnetic resonance contrast agents as biochemical reporters, Curr. Opin. Neurobiol. 13 (2003) 597–602.
[3] R. Weissleder, Liver MR imaging with iron oxides: toward consensus and clinical practice, Radiology 193 (1994) 593–595.
[4] M.K. Yu, J. Park, S. Jon, Targeting strategies for multifunctional nanoparticles in cancer imaging and therapy, Theranostics 2 (2012) 3–44.
[5] H. Lee, E. Lee, K. Kim, et al., Antibiofouling polymer-coated superparamagnetic iron oxide nanoparticles as potential magnetic resonance contrast agents for in vivo cancer imaging, J. Am. Chem. Soc. 128 (2006) 7383–7389.
[6] B.M. Seddon, P. Workman, The role of functional and molecular imaging in cancer drug discovery and development, Br. J. Radiol. 76 Spec No. 2 (2003) S128–S138.
[7] E. Seneterre, P. Taourel, Y. Bouvier, et al., Detection of hepatic metastases: ferumoxides-enhanced MR imaging versus unenhanced MR imaging and CT during arterial portography, Radiology 200 (1996) 785–792.
[8] J.W. Bulte, D.L. Kraitchman, Iron oxide MR contrast agents for molecular and cellular imaging, NMR Biomed. 17 (2004) 484–499.
[9] J. Zhuo, R.P. Gullapalli, AAPM/RSNA physics tutorial for residents: MR artifacts, safety, and quality control, Radiographics 26 (2006) 275–297.
[10] L. Macarini, S. Marini, P. Milillo, et al., Double-contrast MRI (DC-MRI) in the study of the cirrhotic liver: utility of administering Gd-DTPA as a complement to examinations in which SPIO liver uptake and distribution alterations (SPIO-LUDA) are present and in the identification and characterisation of focal lesions, Radiol. Med. 111 (2006) 1087–1102.
[11] R.C. Semelka, J.K. Lee, S. Worawattanakul, et al., Sequential use of ferumoxide particles and gadolinium chelate for the evaluation of focal liver lesions on MRI, J. Magn. Reson. Imaging 8 (1998) 670–674.
[12] R. Weissleder, S. Saini, D.D. Stark, et al., Dual-contrast MR imaging of liver cancer in rats, AJR Am. J. Roentgenol. 150 (1988) 561–566.
[13] J. Ward, J.A. Guthrie, D.J. Scott, et al., Hepatocellular carcinoma in the cirrhotic liver: double-contrast MR imaging for diagnosis, Radiology 216 (2000) 154–162.
[14] N. Bolog, T. Pfammatter, B. Mullhaupt, et al., Double-contrast magnetic resonance imaging of hepatocellular carcinoma after transarterial chemoembolization, Abdom. Imaging 33 (2008) 313–323.
[15] Y. Suto, Y. Shimatani, T. Kato, et al., Double contrast MR imaging with iron colloid and Gd-DTPA in cholangiocellular carcinoma, Acta. Radiol. 35 (1994) 632–633.
[16] F. Zhang, X. Huang, L. Zhu, et al., Noninvasive monitoring of orthotopic glioblastoma therapy response using RGD-conjugated iron oxide nanoparticles, Biomaterials 33 (2012) 5414–5422.
[17] F. Zhang, L. Zhu, X. Huang, et al., Differentiation of reactive and tumor metastatic lymph nodes with diffusion-weighted and SPIO-enhanced MRI. Mol. Imaging Biol., 2012 May 16. [Epub ahead of print].
[18] R.M. Henkelman, P. Hardy, P.Y. Poon, et al., Optimal pulse sequence for imaging hepatic metastases, Radiology 161 (1986) 727–734.
[19] A. Denys, L. Arrive, V. Servois, et al., Hepatic tumors: detection and characterization at 1-T MR imaging enhanced with AMI-25, Radiology 193 (1994) 665–669.
[20] K.D. Hagspiel, K.F. Neidl, A.C. Eichenberger, et al., Detection of liver metastases: comparison of superparamagnetic iron oxide-enhanced and unenhanced MR imaging at 1.5 T with dynamic CT, intraoperative US, and percutaneous US, Radiology 196 (1995) 471–478.
[21] A. Shimizu, K. Ito, S. Koike, et al., Cirrhosis or chronic hepatitis: evaluation of small (< or =2-cm) early-enhancing hepatic lesions with serial contrast-enhanced dynamic MR imaging, Radiology 226 (2003) 550–555.
[22] H. Nakamura, N. Ito, F. Kotake, et al., Tumor-detecting capacity and clinical usefulness of SPIO-MRI in patients with hepatocellular carcinoma, J. Gastroenterol. 35 (2000) 849–855.
[23] B. Misselwitz, MR contrast agents in lymph node imaging, Eur. J. Radiol. 58 (2006) 375–382.
[24] P. Vassallo, C. Matei, W.D. Heston, et al., AMI-227-enhanced MR lymphography: usefulness for differentiating reactive from tumor-bearing lymph nodes, Radiology 193 (1994) 501–506.
[25] R. Weissleder, G. Elizondo, L. Josephson, et al., Experimental lymph node metastases: enhanced detection with MR lymphography, Radiology 171 (1989) 835–839.
[26] S.M. Moghimi, B. Bonnemain, Subcutaneous and intravenous delivery of diagnostic agents to the lymphatic system: applications in lympho-scintigraphy and indirect lymphography, Adv. Drug Deliv. Rev. 37 (1999) 295–312.
[27] K. Suga, Y. Yuan, N. Ogasawara, et al., Localization of breast sentinel lymph nodes by MR lymphography with a conventional gadolinium contrast agent. Preliminary observations in dogs and humans, Acta Radiol. 44 (2003) 35–42.
[28] G. Niu, X. Chen, Why integrin as a primary target for imaging and therapy, Theranostics 1 (2011) 30–47.
[29] X. Chen, Multimodality imaging of tumor integrin alphavbeta3 expression, Mini Rev. Med. Chem. 6 (2006) 227–234.
[30] Y. Ye, X. Chen, Integrin targeting for tumor optical imaging, Theranostics 1 (2011) 102–126.